High-pressure Brillouin scattering in a simple molecular system

2002 J. Phys.: Condens. Matter 14 10657

(http://iopscience.iop.org/0953-8984/14/44/352)

INSTITUTE OF PHYSICS PUBLISHING JOURNAL OF PHYSICS: CONDENSED MATTER

J. Phys.: Condens. Matter **14** (2002) 10657–10664 PII: S0953-8984(02)38462-5

High-pressure Brillouin scattering in a simple molecular system

Hiroyasu Shimizu

Department of Electrical and Electronic Engineering, Faculty of Engineering, Division of Environmental and Renewable Energy System, Graduate School of Engineering, Gifu University, 1-1 Yanagido, Gifu 501-1193, Japan

Received 19 June 2002
Published 25 October 2002
Online at stacks.iop.org/JPhysCM/14/10657

Abstract

Recent developments in high-pressure *in situ* Brillouin spectroscopy of a simple molecular system are reviewed by demonstrating experimental and analytical methods for the study of acoustic velocities in any direction, adiabatic elastic constants, and elastic anisotropy. Detailed applications to solid argon (Ar) are presented, at pressures up to 70 GPa in a diamond anvil cell, using recently developed approaches that combine the method of *in situ* Brillouin spectroscopy, for a single crystal of Ar up to 4 GPa, and the envelope method applied to both longitudinal acoustic and transverse acoustic modes, for recrystallized Ar between 4 and 70 GPa.

1. Introduction

High-pressure Brillouin scattering provides elastic properties of acoustic velocities, adiabatic elastic constants, adiabatic bulk moduli, and elastic anisotropies [1]. With the combination with a diamond anvil cell (DAC), recently such measurements have been successfully performed at very high pressures up to 70 GPa for a simple molecular solid, argon (Ar) [2]. The simple molecular system is central to high-pressure science and a prototype model for condensed matter physics. Since the first high-pressure Brillouin study was carried out for solid hydrogen up to $P = 20$ GPa in 1981 [1], many challenging studies have been carried out on simple molecular solids prepared in the DAC. Polian and his group measured the longitudinal acoustic (LA) velocity for water ice (H_2O; up to $P = 67$ GPa) [3, 4] and solid Ar (up to $P = 33$ GPa) [5] and Kr (up to $P = 30$ GPa) [6], in the backscattering (180°) geometry, without identification of the crystal orientation in the DAC. Shimizu and his group [7] developed *in situ* high-pressure Brillouin spectroscopy which enables us to determine simultaneously acoustic velocities and the orientation of a crystal grown in the DAC. This method reveals elastic properties of pressure-induced single-crystalline H_2S [7, 8], CO_2 [9], H_2O [10–12], CH_4 [13], NH_3 [14], HCl [15], HBr [16], Kr [17], and Ar [2] at room temperature. The Zha and Carnegie group [18] combined high-pressure Brillouin study and x-ray diffraction measurements at

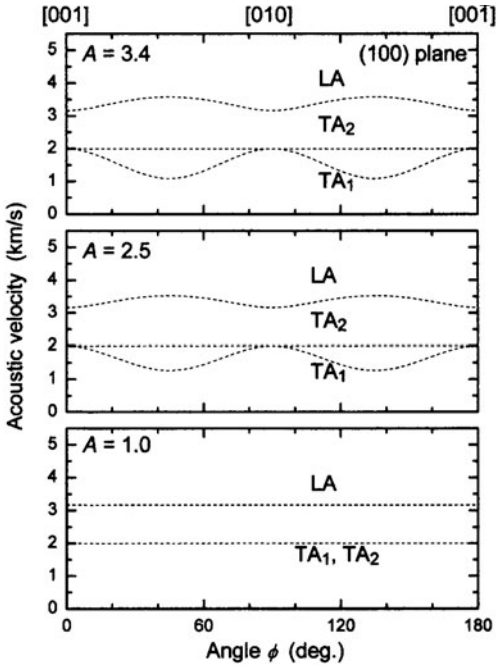

Figure 1. The direction dependences of acoustic velocities for three kinds of elastic anisotropy $A = 1$, 2.5, and 3.4 in a (100) plane of a cubic system.

each applied pressure, and succeeded in determining six elastic constants of solid H_2 up to $P = 24$ GPa at room temperature.

In this paper, we review briefly our *in situ* Brillouin spectroscopy applied to simple molecular systems using a DAC, and present recent Brillouin results for solid Ar up to very high pressure, $P = 70$ GPa, which were accomplished by overcoming the problem of Ar recrystallization in the DAC at $P = 4$ GPa.

2. Experimental and analytical methods of *in situ* Brillouin spectroscopy for simple molecular system

The acoustic velocity (v) for the probed acoustic phonon is critically dependent on the crystal orientation, even for a cubic crystalline system. In figure 1, the direction dependences of the acoustic velocities for LA and two transverse (TA_1, slow; TA_2, fast) modes are shown for three kinds of elastic anisotropy ($A = 1$, 2.5, and 3.4), where A is defined as the square of the ratio of the acoustic velocities of TA_2 to TA_1 propagating along the $\langle 110 \rangle$ direction for a cubic crystalline system having three elastic constants C_{11}, C_{12}, and C_{44} [15]:

$$A = (v_{TA2}/v_{TA1})^2 = 2C_{44}/(C_{11} - C_{12}). \tag{1}$$

We can see that it is necessary to accurately identify the axis orientation of a molecular single crystal grown in a DAC, except for crystals having elastic isotropy ($A = 1$).

A Sandercock tandem Fabry–Perot interferometer [19] was used in the triple-pass arrangement for Brillouin scattering measurements. A 514.5 nm argon-ion laser line (λ_0), providing a single-moded power of about 10–30 mW, was used as the excitation source. The Brillouin frequency shifts ($\Delta\nu$) at 60° and 90° scattering geometries with the DAC are related to the acoustic velocity (v) as follows [1]: $\Delta\nu_{60} = v_{60}/\lambda_0$ and $\Delta\nu_{90} = 2^{1/2}v_{90}/\lambda_0$, where the

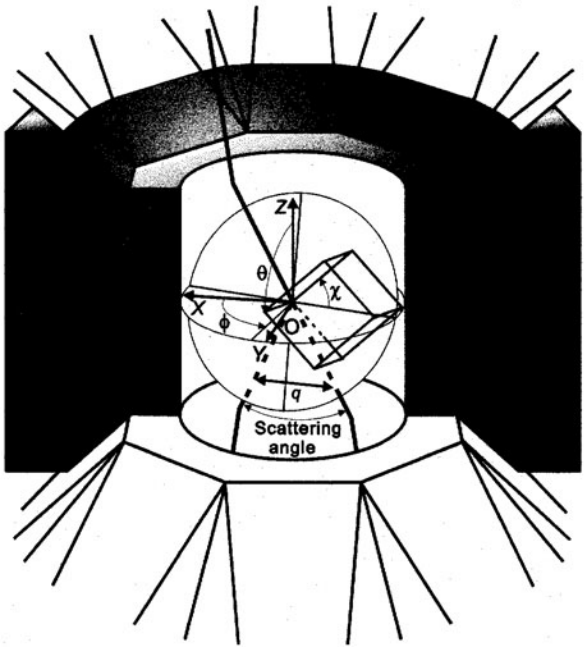

Figure 2. Single-crystal growth of a simple molecular solid in a DAC. The Euler angles (θ, ϕ, χ) indicate the orientation of the cubic crystal in a sample chamber.

wavevector of the probed acoustic phonons is parallel to the culet of the diamond anvils, and v_{60} and v_{90} are independent of the refractive index of the medium. The Brillouin frequency shifts $(\Delta\nu)$ can be calculated theoretically by using the above relations between $\Delta\nu$ and v, and the solution of the elastic equation as follows [7, 9]:

$$\Delta\nu_j = f_j(C_{11}/\rho, C_{12}/\rho, C_{44}/\rho, \theta, \phi, \chi), \tag{2}$$

where the subscript $j(=0, 1, 2)$ indicates LA, TA_1 (slow), and TA_2 (fast) modes, respectively, C_{ij} is the adiabatic elastic constant, ρ is the density, and the Euler angles (θ, ϕ, χ) relate the laboratory frame to the crystal reference frame. In order to determine the three Euler angles and three elastic constants at each pressure, we applied a computerized least-squares fit between the calculated $f_j(\phi_i)$ and experimental frequency shifts $(\phi_i, \Delta\nu_{ji})$ as a function of angle ϕ_i:

$$J = \sum_{ij}[f_j(\phi_i) - \Delta\nu_{ji}]^2, \qquad j = 0, 1, 2, \tag{3}$$

where the sum of square errors is minimized by systematically varying the six parameters until the fit is optimized. As a result, we can determine a complete mapping of the acoustic velocities in the various crystal directions with *in situ* identification (see figure 2) of the crystal orientation (θ, ϕ, χ) at each pressure [7, 9]. Furthermore, we can calculate the acoustic velocity (v_{180}) along the direction perpendicular to the culet of the diamond anvils, which is available to determine the refractive index (n) by using the relation $\Delta\nu_{180} = (2n)v_{180}/\lambda_0$ for 180° Brillouin scattering geometry [1] and the measured 180° Brillouin frequency shift $(\Delta\nu_{180})$.

3. Background for Brillouin studies of solid Ar

The rare-gas argon (Ar) is the third component of dry air by volume, and is among the simplest in nature because of its closed-shell electronic configuration. Rare-gas van der Waals solids

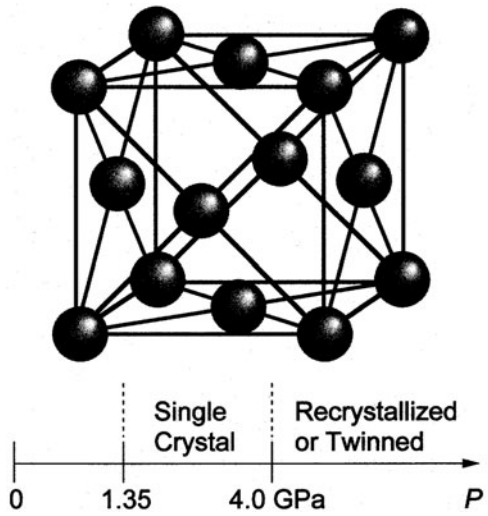

Figure 3. The fcc crystal structure of solid Ar at high pressures and room temperature, and freezing and recrystallizing pressures.

are an important class of materials, providing an ideal system allowing fruitful comparisons between experiments and theoretical calculations. The elastic properties of dense Ar are of fundamental interest in view of its use as the hydrostatic pressure medium for high-pressure research in a DAC and as a component in rocks and the atmospheres of planetary bodies.

At ambient pressure, Ar liquefies at 87.3 K and solidifies in the fcc phase at 83.8 K. At 300 K, the liquid Ar crystallizes into the same phase at about $P = 1.3$ GPa [20, 21]. With increasing pressure, a single crystal of Ar grown in the DAC always recrystallizes to a small group of single crystals at a pressure of about 4 GPa [5, 20]. This crystalline behaviour of solid Ar needs careful experiments above $P = 4$ GPa in order to obtain reliable elastic properties, because the acoustic velocities are sensitive to the crystal direction, as shown in figure 1.

Since Raman and infrared measurements do not show any first-order vibrational spectra for the rare-gas solids, Brillouin scattering experiments become important among the optical techniques available to study them. This Brillouin study gives us information about the acoustic vibrations of the rare-gas single crystals which can yield the determination of the elastic properties. This elasticity provides substantial insight into the nature of bonding in a crystal. For example, the elastic constants reflect the strength of the interatomic forces in a solid, and the Cauchy violation gives a direct measure of the importance of noncentral many-body forces.

Gewurtz and Stoicheff [22] measured the Brillouin scattering of fcc crystalline Ar at 82.3 K and 1 atm, and determined three adiabatic elastic constants. Grimsditch *et al* [5] determined the pressure dependence of three elastic constants up to 33 GPa at 300 K by Brillouin spectroscopy. They measured only the LA mode of solid Ar in a DAC using a backscattering geometry without identification of the crystal orientations, and estimated the envelope curves which correspond to the maximum and the minimum LA velocities for all measured points. (Hereafter, we designate this type of 'max and min' method as the envelope method.)

4. Results and discussion for solid Ar up to P = 70 GPa

For single-crystal Ar at low pressures between 1.3 and 4 GPa, the elastic properties have been studied by using the method of *in situ* Brillouin spectroscopy developed for simple molecular solids.

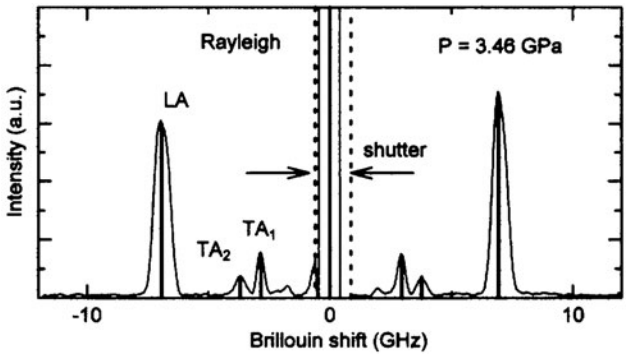

Figure 4. The Brillouin spectrum of solid Ar at $P = 3.46$ GPa. The scattering angle is 60°. LA, TA_2, and TA_1 are Brillouin-shifted signals from longitudinal and fast and slow transverse modes, respectively. The shutter works to attenuate the strong Rayleigh intensity when scanning through its peak.

For recrystallized Ar at high pressures between 4 and 70 GPa, we applied the envelope method to both LA and TA modes; the maximum and the minimum values of the acoustic velocities are estimated by measuring the direction dependence of the acoustic velocities at each pressure, and by using these distributed velocity data we can determine the envelope curves for LA and TA modes. Then, the relations can be derived from theoretical predictions that the maximum LA velocity exists along the ⟨111⟩ direction and is represented by $v_{\mathrm{LA,max}} = [(C_{11} + 2C_{12} + 4C_{44})/(3\rho)]^{1/2}$, and that the minimum LA velocity along the ⟨100⟩ direction is $v_{\mathrm{LA,min}} = (C_{11}/\rho)^{1/2}$; the maximum TA velocity along the ⟨100⟩ direction is $v_{\mathrm{TA,max}} = (C_{44}/\rho)^{1/2}$; and the minimum TA velocity along the ⟨110⟩ direction is $v_{\mathrm{TA,min}} = [(C_{11} - C_{12})/(2\rho)]^{1/2}$.

4.1. In situ Brillouin studies of solid Ar at pressures up to the recrystallization point of 4 GPa

For single-crystal Ar at low pressures between 1.3 and 4 GPa, we were able to observe clearly one LA and two TA modes in the Brillouin spectra (see figure 4). By rotating the DAC at about 10° intervals along the load axis, we measured the ϕ-dependence of the Brillouin frequency shifts (i.e., acoustic velocities) at each pressure, as shown in figure 5. The computerized least-squares fit was applied to determine three elastic constants and Euler angles. We were able to get a best fit to the measured values at each pressure (see figure 5), which yielded, for example, $C_{11}/\rho = 10.2$, $C_{12}/\rho = 7.48$, and $C_{44}/\rho = 4.17$ km^2 s^{-2}, and $\theta = 70.6°$, $\phi = 16.9°$, and $\chi = 24.4°$ at $P = 3.46$ GPa. Once the six parameters were determined, the acoustic velocities could be calculated for all directions. In figure 6 and its inset, the squares of the sound velocities corresponding to $v_{\mathrm{LA,max}}$, $v_{\mathrm{LA,min}}$, $v_{\mathrm{TA,max}}$, and $v_{\mathrm{TA,min}}$ are plotted using solid symbols up to 4 GPa at 300 K.

Next, by use of the equation of state obtained from equation (4), we determined the elastic constants C_{11}, C_{12}, and C_{44} up to 4 GPa, which are plotted by solid symbols up to 4 GPa in the inset of figure 7. They increase almost linearly with increasing pressure. For comparison with the earlier Brillouin study [5], we also show the experimental results, using open symbols. Notable discrepancy can be found in the values for C_{11} and C_{12}, which are due to the earlier measurements being only of the LA velocity for unknown directions of an Ar single crystal.

4.2. Envelope method of Brillouin studies at pressures from 4 to 70 GPa

At pressures above 4 GPa, the probed single crystals in the recrystallized Ar are randomly oriented and, as a result, we should observe a spread of the experimental points for acoustic

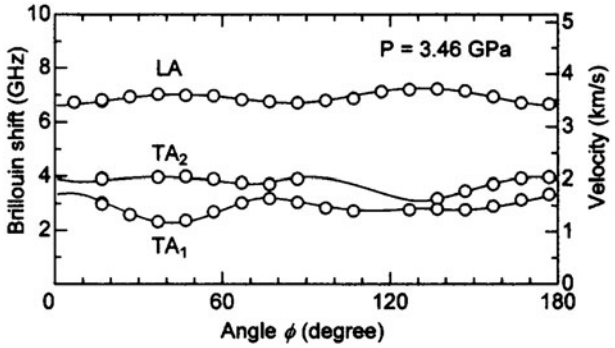

Figure 5. Brillouin frequency shifts and acoustic velocities of LA, TA_2, and TA_1 modes as a function of angle ϕ at 60° scattering geometry for solid Ar at $P = 3.46$ GPa. ϕ shows the angle of rotation about the road axis of the DAC. Open circles indicate experimental points, and the solid curves represent the calculated best-fit velocities.

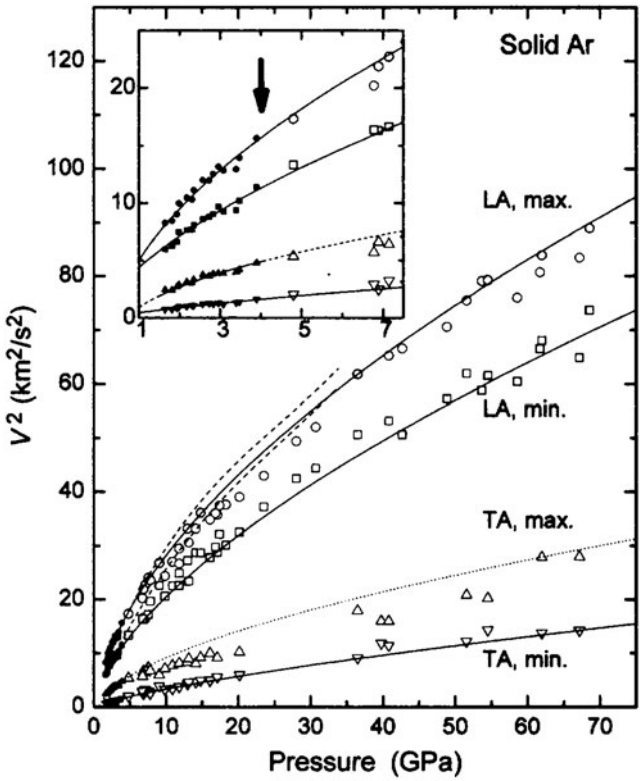

Figure 6. Pressure dependences of the squares of $v_{LA,max}$, $v_{LA,min}$, $v_{TA,max}$, and $v_{TA,min}$. Solid symbols below $P = 4$ GPa (see the inset) indicate experimental points determined directly by the *in situ* Brillouin method. The vertical arrow indicates the Ar recrystallization point at $P = 4$ GPa. Three solid curves show the envelope curves of maximum and minimum velocities of solid Ar up to $P = 70$ GPa, and one dashed curve shows the envelope curve estimated from the three relations of the above three envelope curves. The two broken curves show the earlier data [5] for envelope curves for the LA mode up to 33 GPa.

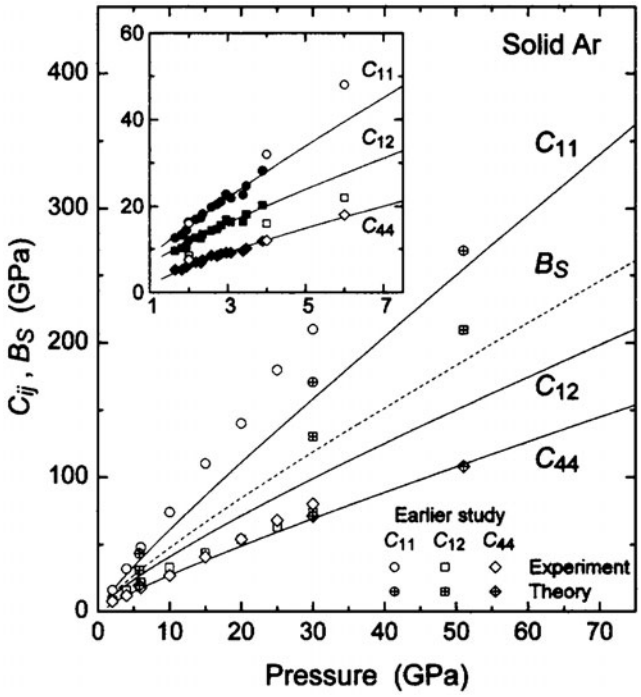

Figure 7. Pressure dependences of three adiabatic elastic constants and the adiabatic bulk modulus (B_S) for solid Ar up to 70 GPa at 300 K: present studies: solid curves (C_{11}, C_{12}, and C_{44}) and dashed curve (B_S); earlier experiments to 33 GPa [5]: open symbols; theoretical calculations to 51 GPa [5]: open symbols with crosses. The solid symbols in the inset show the present results obtained by the *in situ* Brillouin method between 1.3 and 4 GPa.

velocities. We estimated the maximum and the minimum velocities of observed LA and TA modes in many different runs by measuring the direction dependence of the acoustic velocities at each pressure. In figure 6, experimental results are plotted using open symbols for LA and TA modes up to 70 GPa. We determined the envelope curves for LA and TA modes self-consistently by extrapolating the reliable low-pressure data and by interpolating the high-pressure data around $P = 4$ GPa. Since the Brillouin signal for the maximum velocity of the TA_2 mode corresponding to $(C_{44}/\rho)^{1/2}$ was hardly observed, the value of $v_{TA,max}$ could not be precisely estimated. However, it is sufficient to determine three elastic constants by using three relations for $v_{LA,max}$, $v_{LA,min}$, and $v_{TA,min}$. The results obtained can determine the value of $v_{TA,max} = (C_{44}/\rho)^{1/2}$, and the squares of their velocities are reasonably well represented by the dashed curve in figure 6. The pressure dependences of these estimated C_{11}/ρ, C_{12}/ρ, and C_{44}/ρ reveal the acoustic velocities for all directions of solid Ar up to 70 GPa. To compare with the earlier study up to 33 GPa, we show the Grimsditch *et al* envelope curves for the LA mode as two broken curves in figure 6 [5]; these were calculated from their data for elastic moduli. The agreement for the square of $v_{LA,max}$ is fairly good, but the disagreement for the square of $v_{LA,min}$ is remarkable.

Next, we determined the equation of state of solid Ar between 4 and 70 GPa by using equation (4), below, with $\gamma(P) = C_P/C_V = B_S/B_T$ and the bulk sound velocity, $V_B = [(C_{11} + 2C_{12})/(3\rho)]^{1/2}$:

$$\rho(P) = \rho(P_r) + \int_{Pr}^{P} (\gamma/V_B^2)\,\mathrm{d}P \tag{4}$$

and compared with x-ray data [20, 23]. The agreement is very good, which indicates that our envelope method is self-consistent and applies nicely. The present results for $\rho(P)$ yielded the determination of C_{11}, C_{12}, C_{44}, and B_S as shown in figure 7. They increase monotonically with increasing pressure, and indicate $C_{11} = 340$ GPa, $C_{12} = 199$ GPa, $C_{44} = 145$ GPa, and $B_S = 246$ GPa at $P = 70$ GPa. It is surprising that at pressures above 43 GPa, B_S for rare-gas solid Ar shows larger values than that of bcc iron ($\sim$160 GPa) at 1 atm and 300 K. There is no evidence of structural phase transformation over a wide range of pressure to 70 GPa, and Born's stability conditions are satisfied. For comparison with the earlier Brillouin study to 33 GPa [5], we also show those experimental results (open symbols) and theoretical calculations (open symbols with crosses) in figure 7. A remarkable discrepancy can be found for C_{11} and C_{12}, which are due to features of the earlier study: (1) the uncertainty of the envelope curves determined by the use of only the LA mode based on the measurement of nv in the backscattering geometry and (2) the assumption that $B_S/B_T = \gamma = 1$ at all pressures. The theoretical calculations up to $P = 51$ GPa [5] remain at variance with the present experimental results; the self-consistent phonon calculations were performed using a pair potential proposed by Aziz and Chen [24].

5. Summary

The present study has provided the first complete results for elastic properties of the rare-gas solid Ar at very high pressures up to 70 GPa, which were accomplished by overcoming the problem of Ar recrystallization in the DAC at $P = 4$ GPa. These reliable and wide-ranging elastic properties provide strong constraints on the best construction of interatomic potentials which are essential for obtaining thermodynamic quantities for the ideal solid Ar at high pressures and temperatures.

References

[1] Shimizu H, Brody E M, Mao H K and Bell P M 1981 *Phys. Rev. Lett.* **47** 128
[2] Shimizu H, Tashiro H, Kume T and Sasaki S 2001 *Phys. Rev. Lett.* **86** 4568
[3] Polian A and Grimsditch M 1983 *Phys. Rev.* B **27** 6409
[4] Polian A and Grimsditch M 1984 *Phys. Rev. Lett.* **52** 1312
[5] Grimsditch M, Loubeyre P and Polian A 1986 *Phys. Rev.* B **33** 7192
[6] Polian A, Besson J M, Grimsditch M and Grosshans W A 1989 *Phys. Rev.* B **39** 1332
[7] Shimizu H and Sasaki S 1992 *Science* **257** 514
[8] Sasaki S and Shimizu H 1995 *J. Phys. Soc. Japan* **64** 3309
[9] Shimizu H, Kitagawa T and Sasaki S 1993 *Phys. Rev.* B **47** 11 567
[10] Shimizu H, Ohnishi M, Sasaki S and Ishibashi Y 1995 *Phys. Rev. Lett.* **74** 2820
[11] Shimizu H, Nabetani T, Nishiba T and Sasaki S 1996 *Phys. Rev.* B **53** 6107
[12] Shimizu H 1998 *Rev. High Pressure Sci. Technol.* **7** 1124
[13] Shimizu H, Nakashima N and Sasaki S 1996 *Phys. Rev.* B **53** 111
[14] Kume T, Daimon M, Sasaki S and Shimizu H 1998 *Phys. Rev.* B **57** 13 347
[15] Shimizu H, Kamabuchi K, Kume T and Sasaki S 1999 *Phys. Rev.* B **59** 11 727
[16] Shimizu H, Kanazawa M, Kume T and Sasaki S 1999 *J. Chem. Phys.* **111** 10 617
[17] Shimizu H, Saitoh N and Sasaki S 1998 *Phys. Rev.* B **57** 230
[18] Zha C S, Duffy T S, Mao H K and Hemley R J 1993 *Phys. Rev.* B **48** 9246
[19] Mock R, Hillebrands B and Sandercock R 1987 *J. Phys. E: Sci. Instrum.* **20** 656
[20] Finger L W, Hazen R M, Zou G, Mao H K and Bell P M 1981 *Appl. Phys. Lett.* **39** 892
[21] Datchi F, Loubeyre P and LeToullec R 2000 *Phys. Rev.* B **61** 6535
[22] Gewurtz S and Stoicheff B P 1974 *Phys. Rev.* B **10** 3487
[23] Ross M, Mao H K, Bell P M and Xu J A 1986 *J. Chem. Phys.* **85** 1028
[24] Aziz R A and Chen H H 1977 *J. Chem. Phys.* **67** 5719